Research Article

OPEN ACCESS

SCC Publishing
Michelets vei 8 B
1366 Lysaker Norway

ISSN: 2703-9072

Correspondence:
cohler@post.harvard.edu

Vol. 6.4 (2026)
pp. 137–150

A Statistically Significant Positive Recent-Window Trend in the Atmospheric Input Isotopic Signature $\delta^{13}C_I$ Falsifies the Fossil-Fuel Dominance Hypothesis for Rising Atmospheric CO_2

Jonathan Cohler[1]*, *Willie Soon*[2]

[1]*Cohler & Associates, Inc., Lexington, MA 02420, USA*
[2]*Institute of Earth Physics and Space Science, 9400 Sopron, Hungary*

Abstract

We test the prediction that fossil-fuel dominance of the recent CO_2 rise, the hypothesis central to IPCC assessment [3] and reasserted in recent carbon-cycle attribution analyses [6], should drive the net atmospheric input isotopic signature $\delta^{13}C_I$ strongly negative during the highest-emissions window. Applying Equation 13 of Koutsoyiannis (2024) [13] with the fixed-$\Delta[CO_2]$ technique to the Francey et al. (1999) [7] Law Dome, firn, and Cape Grim Air Archive record, we find the 1977–1996 trend in $\delta^{13}C_I$ to be +2.94‰ per decade against a Hurst–Kolmogorov 95% envelope of $[-1.26, +1.24]$‰ per decade, with $p < 10^{-4}$. The trend is statistically significant, its sign is opposite to the fossil-dominance prediction, and its magnitude is more than twice the upper envelope bound. The fossil-dominance hypothesis is falsified on this record. The positive sign is consistent with a growing ocean-outgassing contribution under recent warming, the mechanism developed in Cohler & Soon (2026b) [5].

Keywords: atmospheric CO_2; carbon isotopes; $\delta^{13}C$; Keeling plot; Law Dome; fossil-fuel attribution; Hurst–Kolmogorov; falsification; Suess effect

Submitted 2026-09-20, Accepted 2026-11-16. https://doi.org/10.53234/scc202612/07

1. Introduction

Fossil-fuel combustion releases carbon that is isotopically much lighter than the carbon already in the atmosphere. If fossil combustion were the dominant source of the 1977–1996 atmospheric CO_2 rise, the isotopic signature of what the atmosphere is being fed would have to be shifting toward that light value during the highest-emissions years. We measure that signature directly from the ice-core, firn, and air-archive record and show that it shifts in the opposite direction, by a large margin and with high statistical confidence. The fossil-dominance hypothesis is falsified on the record.

The carbon-isotope notation used throughout is as follows. The $\delta^{13}C$ value of a sample on the VPDB (Vienna Pee Dee Belemnite) scale is

$$\delta^{13}C_{VPDB} = \left(\frac{R_{sample}}{R_{VPDB}} - 1 \right) \times 1000 \text{ ‰} \quad (1)$$

with $R = {}^{13}C/{}^{12}C$ and $R_{VPDB} = 0.0111802$. The symbol $\delta^{13}C_I$ denotes the flux-weighted mean $\delta^{13}C_{VPDB}$ of the net atmospheric CO_2 input over a specified interval, extracted from the Keeling-plot construction defined in Equation (5). It is the isotopic signature of the net input flux, not of the atmospheric reservoir.

The claim that essentially all of the observed post-industrial rise in atmospheric CO_2 originates from fossil-fuel combustion is central to IPCC assessment [3] and has been reasserted in recent carbon-cycle attribution analyses aligned with that framework [6]. This claim yields a testable prediction about the isotopic composition of the net atmospheric input through the Keeling-plot construction [9]. Fossil combustion releases carbon at approximately −28‰ on the VPDB scale [1], inherited from the C3-photosynthesis signature of the ancient source biomass [12]; ocean-outgassed CO_2 after equilibrium fractionation with surface dissolved inorganic carbon (DIC) carries a signature near −8‰ [14, 17]; the modern atmospheric reservoir sits near −8.5‰ [10]. The progressive isotopic lightening of atmospheric CO_2 has been speculated to derive from the addition of fossil-fuel carbon to the atmosphere, a conjecture known as the "Suess effect." A source progressively dominated by fossil combustion must mathematically drive the flux-weighted mean signature $\delta^{13}C_I$ of the net atmospheric input toward −28‰, in proportion to the fossil share of the net flux.

Two complementary isotopic falsifications of this prediction already exist. Koutsoyiannis (2024) [13] shows that $\delta^{13}C_I$ is stationary at -13.2 ± 0.2‰ across the full instrumental period and across a five-century proxy extension back to the Little Ice Age, about 15‰ less negative than the fossil signature. Cohler & Soon (2026a) [4] combines that stationary intercept with the mass partition equation and the standard $\delta^{13}C$ values from the peer-reviewed literature to obtain the algebraic bound $f \leq 0.013$ on the fossil fraction of the net atmospheric addition. Section 7.1 develops both results.

This paper establishes a third complementary falsification by testing the trend prediction. Between 1977 and 1996, global annual fossil-fuel emissions rose from approximately 5 to approximately 6.6 GtC/yr [8], the fastest sustained rise within the interval covered by the Law Dome record used here. Under fossil dominance the recent-window trend in $\delta^{13}C_I$ must be negative in sign, large in magnitude on the scale set by the fossil-natural signature gap, and statistically distinguishable from the noise background of the extraction. Section 2.1 develops this prediction formally.

We test this prediction directly. Section 2 states the fossil-dominance prediction and its alternative in operational form. Section 3 describes the Koutsoyiannis (2024) [13] Equation 13 extraction of $\delta^{13}C_I$ and the Hurst–Kolmogorov Monte Carlo test used to assess significance. Section 4 identifies the primary data source, Francey et al. (1999) [7], and two alternative treatments that address data-provenance robustness. Section 5 reports the primary falsification result on the Francey data, and its robustness across the alternative treatments. Section 6 documents that the one treatment on which the falsification appears to fail (the Rubino et al. (2013) [15] revision) fails only through an endpoint truncation with no measurement-chain justification. Restoring the truncated years recovers the significant result. Section 7 places the finding in the context of the other two isotopic falsifications, identifies the physical mechanism the observed sign implies, and addresses the downstream literature consequences. Section 8 concludes.

1.1 Glossary

VPDB Vienna Pee Dee Belemnite, the international reference standard for carbon-isotope ratios.

$\delta^{13}C$ Per-mil deviation of the ${}^{13}C/{}^{12}C$ ratio of a sample from the VPDB standard, Equation (1).

$\delta^{13}C_I$ Flux-weighted mean $\delta^{13}C$ of the net atmospheric CO_2 input over a specified interval; extracted from Equation (5).

DIC Dissolved inorganic carbon: the sum of dissolved CO_2, bicarbonate, and carbonate in seawater.

CGAA Cape Grim Air Archive: the CSIRO collection of whole-air samples in 35-litre stainless-steel flasks collected at Cape Grim, Tasmania, since 1978.

Keeling plot A regression of $\delta^{13}C$ on $1/[CO_2]$ whose intercept gives the flux-weighted mean signature of the net atmospheric input over the fit window.

Hurst–Kolmogorov noise A long-range persistent stochastic model (Hurst exponent $H > 0.5$) used to size the noise envelope for trend tests on geophysical series.

Fossil-dominance hypothesis The hypothesis that essentially all (fossil fraction $f \approx 1$) of the net atmospheric CO_2 addition since the industrial period originates from fossil-fuel combustion.

OLS Ordinary least squares.

2. The Falsification Structure

2.1 The fossil-dominance prediction

The mass partition equation for the flux-weighted mean signature of the net atmospheric CO_2 input (Cohler & Soon (2026a) [4]) follows from mass conservation alone and is

$$\delta^{13}C_I(t) = f(t)\,\delta^{13}C_F + \big(1 - f(t)\big)\,\delta^{13}C_N(t) \tag{2}$$

where $f(t)$ is the fossil fraction of the net atmospheric input at time t, $\delta^{13}C_F \approx -28‰$ is the standard $\delta^{13}C$ value for fossil-fuel-generated CO_2 from the peer-reviewed literature, and $\delta^{13}C_N(t)$ is the flux-weighted mean signature of the non-fossil-fuel net input, bounded above by the standard ocean-outgassing $\delta^{13}C$ value near $-8‰$ and below by the observed intercept itself near $-13.2‰$. By definition, $f(t) \in [0, 1]$ and the non-fossil-fuel fraction is $1 - f(t)$ which is also $\in [0, 1]$: Equation (2) is a mass partition, not a modeling choice. Operationally, $\delta^{13}C_N$ is defined by this partition: it is the signature of the non-fossil-fuel complement, i.e., the weighted signature of whatever net flux crossed the atmospheric boundary in either direction that was not of fossil-fuel origin. It is not a statement about the gross directional balance of the biosphere or ocean, nor about any particular reservoir or whether one is a net source or sink during the interval.

If $f(t)$ grows monotonically with fossil-fuel emission rate, and if the fossil-fuel emission rate accelerated over the recent window as documented by Friedlingstein et al. (2026) [8], then Equation (2) implies

$$\left.\frac{\mathrm{d}\,\delta^{13}C_I}{\mathrm{d}t}\right|_{\text{recent}} = \big(\delta^{13}C_F - \delta^{13}C_N\big)\frac{\mathrm{d}f}{\mathrm{d}t} + (1 - f)\frac{\mathrm{d}\,\delta^{13}C_N}{\mathrm{d}t} \tag{3}$$

The first term is unambiguously negative for any growing fossil share, because $\delta^{13}C_F - \delta^{13}C_N$ lies between approximately $-20‰$ (at $\delta^{13}C_N \approx -8‰$) and $-14.8‰$ (at $\delta^{13}C_N \approx -13.2‰$), and $\mathrm{d}f/\mathrm{d}t > 0$ during the emissions ramp.

The second term, $\mathrm{d}\delta^{13}C_N/\mathrm{d}t$, is empirically bounded by the preindustrial sclerosponge record. Prior to the industrial era (before approximately 1850), fossil-fuel emissions are negligible by any accounting, so the fossil-dominance framework itself requires $f \approx 0$ preindustrial, and Equation (2) then reduces to $\delta^{13}C_I = \delta^{13}C_N$. Böhm et al. (2002) [2], analyzed by Koutsoyiannis (2024) [13], establishes $\delta^{13}C_I = -13.2 \pm 0.2‰$ stationary across the five-century Caribbean sclerosponge window. Under fossil dominance this stationarity transfers directly to $\delta^{13}C_N$, which must therefore satisfy

$$|\Delta\delta^{13}C_N| \le 0.4\ ‰ \text{ over } 500\ \text{yr}, \quad \text{so} \quad \left|\frac{\mathrm{d}\delta^{13}C_N}{\mathrm{d}t}\right| \le 0.008\ ‰/\text{decade} \tag{4}$$

for any drift sustained over the sclerosponge window. The physical basis for this stationarity is the ocean dissolved-inorganic-carbon reservoir of approximately 38,000 GtC, nearly fifty times the atmospheric CO_2 reservoir of approximately 800 GtC. The ocean's own $\delta^{13}C$ changes only on

multi-millennial timescales, set by that reservoir mass divided by the net isotopic turnover flux, and the ocean-outgassing signature it imprints on the atmosphere inherits that multi-millennial slowness. No mechanism in the fossil-dominance framework accelerates $\delta^{13}C_N$ drift during the recent window, so the preindustrial bound of ≈ 0.01‰ per decade carries through to the 1977–1996 test window.

Combining the two bounds, the second term in Equation (3) is at most approximately 1% of the first-term magnitude during any emissions ramp and cannot alter the first-term sign. Under fossil dominance, therefore, the sign of $d\delta^{13}C_I/dt$ in the recent window must be negative.

A recent-window trend that is positive, or that is negative but of magnitude less than the noise envelope, is inconsistent with fossil dominance. A recent-window trend that is significantly positive is affirmatively consistent with a growing non-fossil-fuel contribution whose flux-weighted mean signature is less negative (heavier in ^{13}C, i.e., carrying a larger $^{13}C/^{12}C$ ratio) than the current $\delta^{13}C_I$, which under Equation (2) requires $\delta^{13}C_N$ to move toward the standard ocean-outgassing $\delta^{13}C$ value of -8‰, i.e., an increasing ocean-outgassing contribution to the net input.

2.2 The alternative prediction

The alternative hypothesis under test is that the net atmospheric addition is dominated by non-fossil-fuel fluxes whose partition responds to surface warming. Under van't Hoff kinetics, surface-ocean pCO_2 responds to a surface temperature T with a sensitivity $\partial \ln pCO_2/\partial T \approx 0.0423\ K^{-1}$, acting on the whole surface ocean essentially instantly [5]. Under Arrhenius kinetics with $Q_{10} \approx 1.5$ (the factor by which the respiration rate changes per 10 K of warming), biosphere respiration responds to warming with sensitivity $d \ln R/dT \approx 0.0405\ K^{-1}$, but buffered by thermal inertia and biological turnover on decadal timescales. The ocean fraction of the enhanced non-fossil-fuel flux therefore grows relative to the biosphere fraction during the fastest-warming subperiod, and the flux-weighted mean $\delta^{13}C_N$ shifts toward the less-negative standard ocean-outgassing $\delta^{13}C$ value. Under this mechanism, Equation (2) predicts a positive recent-window trend in $\delta^{13}C_I$, with $f \approx 0$ and $d\delta^{13}C_N/dt > 0$.

Sections 3–5 test which prediction the data actually satisfies.

3. Method

3.1 Koutsoyiannis's Equation 13 with the fixed-$\Delta[CO_2]$ technique

Let $\delta^{13}C(t)$ denote the atmospheric $\delta^{13}C_{VPDB}$ value of CO_2 at time t (the composition of the atmospheric reservoir, as measured at the sampling site), and let $C(t)$ denote the atmospheric CO_2 mole fraction at time t in ppm (on the WMO X93 mole-fraction calibration scale). Conservation of the light and heavy isotope masses in the atmospheric reservoir yields the following expression for the flux-weighted mean signature of the net input over the interval $[t_0, t]$:

$$\delta^{13}C_I(t_0, t) = \frac{\delta^{13}C(t)\,C(t) - \delta^{13}C(t_0)\,C(t_0)}{C(t) - C(t_0)} \tag{5}$$

Equation (5) is Equation 13 of Koutsoyiannis (2024) [13]. It requires no source or sink model and reduces to the intercept of a Keeling plot fit over the same interval in the small-ratio limit.

Equation (5) captures every gross and net isotopic process by construction, including photosynthesis-vs-respiration fractionation imbalances, shifting C3/C4 plant productivity ratios, and ocean-uptake-vs-outgassing fractionation differences. Gross bidirectional exchange whose forward and reverse legs cancel in mass contributes zero to the denominator $C(t) - C(t_0)$; any imbalance in $\delta^{13}C$ between the forward and reverse legs, multiplied by the gross flux, enters the numerator as a net isotopic input with a specific signature. Nothing in the extraction assumes equilibrium or balanced gross fluxes.

The pointwise series is constructed by choosing, for each endpoint t_i, the most recent prior time $t_j < t_i$ satisfying $|C(t_i) - C(t_j)| \geq \sigma_{[CO_2]}$, where $\sigma_{[CO_2]}$ is the record-wide standard deviation of concentration. This holds the extraction denominator close to the record-wide scale and stabilizes the extraction noise floor across the record. Endpoints for which no admissible t_j exists are excluded.

3.2 Hurst–Kolmogorov noise model

Geophysical series typically carry long-range persistence, and the classical white-noise significance test underestimates the noise envelope for a trend statistic on such a series. The Hurst–Kolmogorov (H–K) framework replaces the white-noise assumption with a stationary Gaussian series of autocovariance $\gamma(k) = \frac{1}{2}\left[|k-1|^{2H} - 2|k|^{2H} + |k+1|^{2H}\right]$ characterized by a single Hurst exponent $H \in [0.5, 1)$, so that the sample-mean variance scales as $n^{-(2-2H)}$ rather than as n^{-1}. The H–K null is a long-range persistent stochastic model, not a white-noise null; it is used precisely because geophysical series carry long-range persistence that inflates the trend-test noise envelope relative to the white-noise case, so a rejection against H–K is a stronger statement than a rejection against white noise. The test statistic is the trend of $\delta^{13}C_I$ on year over the target subperiod, expressed in ‰ per decade.

We estimate H from the observed $\delta^{13}C_I$ series by rescaled-range (R/S) analysis over chunk sizes from six years to half the series length, clamped to $[0.5, 0.99]$. The estimate is made on the full series, which includes the recent-window subperiod under test. If the recent-window trend is a real physical signal rather than a realization of H–K noise, its inclusion in the R/S regression inflates the estimated H; the null envelope generated at that inflated H is correspondingly wider than the envelope generated from the pre-recent portion of the series alone. This choice is therefore conservative for a positive finding: any rejection of the null under a full-series H would be at least as strong under an H estimated from the noise-only portion.

We then generate $N = 10\,000$ synthetic fractional Gaussian noise realizations at the estimated H using the Davies–Harte spectral algorithm. Each synthetic realization has the same length as the observed $\delta^{13}C_I$ series (Section 3.1), rescaled to the observed sample mean and standard deviation. The test statistic on each realization is the ordinary-least-squares (OLS) slope over the same recent-window subperiod indices as the observed trend, expressed in ‰ per decade. The 95% envelope is the $[2.5, 97.5]$ percentile range of the synthetic trend distribution. The two-sided p-value is $2\min\{P(T \geq T_{obs}), P(T \leq T_{obs})\}$. An observed trend outside the envelope rejects the H–K null at 5%. This is the same test structure Koutsoyiannis (2024) [13] reports for the subperiod trends in his own analysis.

4. Data

4.1 Primary data source: Francey et al. 1999

The primary data source is Francey et al. (1999) [7], which combines Law Dome DE08, DE08-2, and DSS ice-core samples (58 accepted post-quality-control values spanning 1006–1978), DE08-2 firn air samples (14 measurements spanning 1976–1993), and the Cape Grim Air Archive (CGAA) tank samples (41 tanks spanning 1978–1996), all measured on the same CSIRO Global Atmospheric Sampling Laboratory (GASLAB) MAT252 mass spectrometer against the same CG92 air-standard scale. Ice-core CO_2 concentrations are on the WMO X93 mole-fraction calibration scale. The Francey compilation is the original source dataset for the atmospheric $\delta^{13}C$-CO_2 record over the past millennium and is cited as such throughout the downstream carbon-cycle literature.

4.2 Alternative treatments for robustness

To test the robustness of the primary result to data source, we apply the identical Equation (5) procedure to two additional treatments.

The first alternative is the Rubino et al. (2013) [15] revision (reissued in Rubino et al. (2019) [16]), which reanalyzed the Law Dome ice and firn samples with updated laboratory procedures but did not include the Cape Grim Air Archive tanks. The Rubino record spans 1006–1993 and is the currently cited authoritative Law Dome $\delta^{13}C$-CO_2 dataset in the IPCC AR6 carbon cycle chapter [3] and in the NOAA/WDS Paleoclimatology archive.

The second alternative is the Rubino record extended with the three CGAA tank measurements for 1994, 1995, and 1996 from Francey's Table 1. These three samples belong to the same Cape Grim Air Archive and the same CSIRO GASLAB measurement chain as the 1978–1993 CGAA tanks that Francey published and Rubino omitted. All CGAA tanks were collected at Cape Grim in 35-litre stainless-steel flasks, measured on the same MAT252 mass spectrometer with the same MT Box-C admission scheme and calibrated on the same CG92 air-standard scale used for every ice and firn sample in Rubino's revision. Their exclusion from the Rubino et al. papers is not a measurement-chain decision but a source-medium scope decision. Table 1 summarizes the three treatments.

Table 1: The three data treatments applied to Equation (5). All measurements are from the same CSIRO GASLAB MAT252 measurement chain calibrated on the CG92 air-standard scale.

Treatment	Time span	Ice + firn	CGAA	Endpoint
Francey et al. (1999) [7] (primary)	1006–1996	Yes	Yes (1978–1996)	1996
Rubino 2013/2019 revision	1006–1993	Yes	No	1993
Rubino + CGAA 1994–1996	1006–1996	Yes	Yes (1994–1996)	1996

5. Results

The recent-window subperiod used throughout this section is 1977–1996. This subperiod carries the sharpest sustained rise in global fossil-fuel emissions within the record (approximately 5 to 6.6 GtC/yr per Friedlingstein et al. (2026) [8]), and is therefore the subperiod on which the fossil-dominance prediction is strongest and most falsifiable.

5.1 Primary result: falsification on Francey 1999

The pointwise $\delta^{13}C_I$ series constructed from the Francey et al. (1999) [7] data by Equation (5) covers 1873–1996 with 124 points (the Francey curve in Figure 1). The recent-window subperiod (1977–1996) contains 20 of those points. The observed linear trend on the recent-window subperiod is

$$\left.\frac{\mathrm{d}\,\delta^{13}C_I}{\mathrm{d}t}\right|_{1977\text{–}1996}^{\text{Francey}} = +2.94\ ‰/\text{decade} \tag{6}$$

The rescaled-range Hurst exponent of the full $\delta^{13}C_I$ series is $H = 0.921$, indicating strong persistence. The H–K Monte Carlo with 10 000 replicates of fractional Gaussian noise at that H yields a 95% envelope for the recent-window trend of $[-1.26, +1.24]$‰ per decade. The observed value +2.94‰ per decade sits outside the envelope, at more than twice its upper bound. The two-sided p-value is less than 10^{-4}.

The observed trend is (i) highly statistically significant against the H–K null at $p < 10^{-4}$ (above 99.99% confidence), (ii) positive in sign, and (iii) of magnitude more than twice the upper bound of the null envelope. Comparing against the fossil-dominance prediction set out in Section 2.1: the observed sign is opposite to the prediction, and the observed magnitude exceeds the upper bound

of the noise envelope in that opposite direction by a factor of 2.4. The fossil-dominance hypothesis is falsified.

Comparing against the ocean-outgassing prediction set out in Section 2.2: the observed sign is the predicted sign, and the observed magnitude is of the order of magnitude expected for a decadal shift in $\delta^{13}C_N$ under the temperature-driven mechanism.

5.2 Robustness across treatments

Figure 1 shows the $\delta^{13}C_I$ series computed by Equation (5) on the three treatments. The Rubino and Rubino+CGAA series overlap essentially perfectly across the shared window because they share the same ice+firn base and differ only by the three appended CGAA years. The Francey series shows the same broad structure but sits systematically 1–2‰ less negative than the Rubino-based series across much of the 1900–1975 interval, reflecting the different underlying weighting of ice, firn, and Cape Grim tank samples entering the annual means fed to Equation (5) and the differences between Francey's original ice-and-firn measurements and Rubino's revised values on the same samples. The two treatments that extend to 1996 (Francey and Rubino+CGAA) end at similar recent-window values; the Rubino-alone treatment terminates at 1993, three years before the sharpest phase of the recent upward reversal.

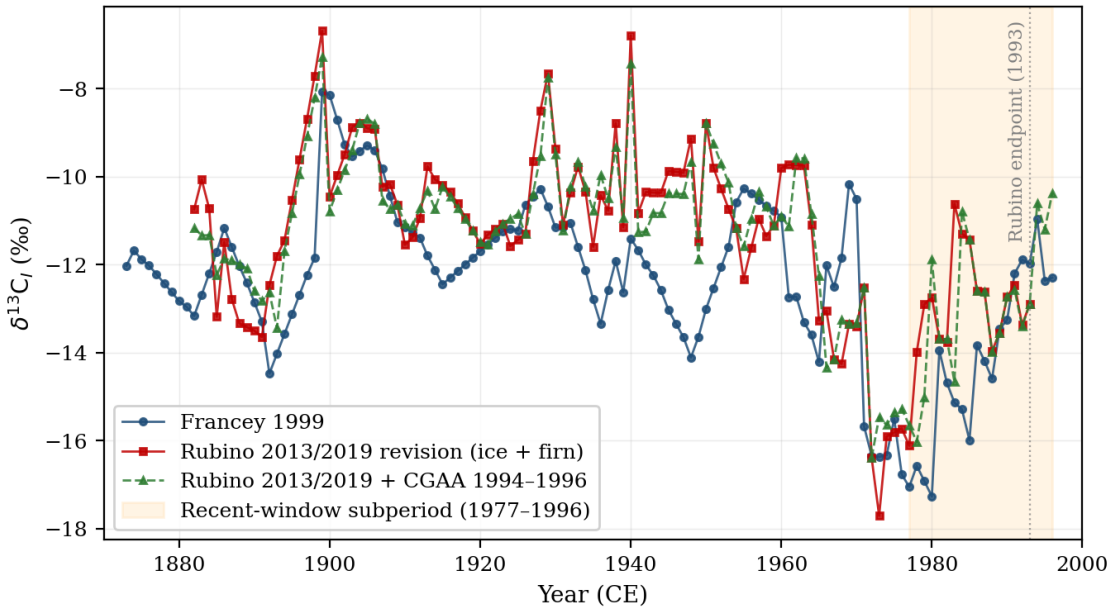


Figure 1: Pointwise input isotopic signature $\delta^{13}C_I$ from Equation (5) with the fixed-$\Delta[CO_2]$ technique for the three data treatments. Rubino and Rubino+CGAA overlap through 1993 by construction (identical ice-and-firn base) and differ only in the three added CGAA years. Francey shares the same broad structure but sits systematically 1–2‰ less negative than the Rubino-based series across much of 1900–1975, reflecting the different underlying weighting of ice, firn, and CGAA samples entering the annual means and the differences between Francey's original and Rubino's revised ice-and-firn measurements. Shaded band: recent-window subperiod used for the falsification test.

The large-amplitude excursions visible in Figure 1 before approximately 1960 are extraction-noise excursions. The pointwise $\delta^{13}C_I$ defined by Equation (5) is a ratio of differences in $C \cdot \delta^{13}C$ and in C; its noise amplitude grows sharply as $C(t)$ and $C(t_0)$ become close, so the extraction is numerically unstable in exactly those regimes where fossil-fuel emissions were small enough that the inter-year concentration spread approached the measurement noise floor. The fixed-$\Delta[CO_2]$ stabilization specified in Section 3.1, which requires $|C(t_i) - C(t_j)| \geq \sigma_{[CO_2]}$ for each endpoint, is precisely the technique that handles this. From approximately 1960 onward the concentration spread between admissible endpoints is sufficient for the extraction to stabilize and the underlying

signal in $\delta^{13}C_I$ to emerge. The stabilized signal shows a declining subperiod from approximately 1960 through the mid-1970s followed by the sustained rise from 1977 to 1996; both features are consequences of the single physical mechanism developed in Section 7.2. The 1977–1996 subperiod used for the falsification test is the first interval in the Francey record on which the signal is both stable in the extraction sense and testable at statistical significance against the H–K null.

Table 2 reports the recent-window test result on each treatment. Figure 2 shows the trend against the H–K null distribution for each.

Table 2: Recent-window (1977–endpoint) trend in $\delta^{13}C_I$ and H–K test result. The H–K envelope columns give the $[2.5, 97.5]$ percentile range of the recent-window trend distribution over 10 000 synthetic fractional-Gaussian-noise realizations at the estimated Hurst exponent H. The sign of the trend is positive on every treatment, contradicting the fossil-dominance prediction (Section 2.1) throughout. The trend is statistically significant against the H–K null on the primary data (Francey 1999) and on Rubino + CGAA. The Rubino-alone treatment is examined in Section 6.

Treatment	Endpoint	n	H	Trend (‰/dec)	H–K envelope (‰/dec)	p	Verdict
Francey 1999 (primary)	1996	20	0.921	+2.94	$[-1.26, +1.24]$	$< 10^{-4}$	**falsifies fossil**
Rubino 2013/2019 revision	1993	17	0.930	+0.67	$[-1.50, +1.54]$	0.40	sign consistent
Rubino + CGAA 1994–96	1996	20	0.955	+1.81	$[-1.01, +1.01]$	$< 10^{-4}$	**falsifies fossil**

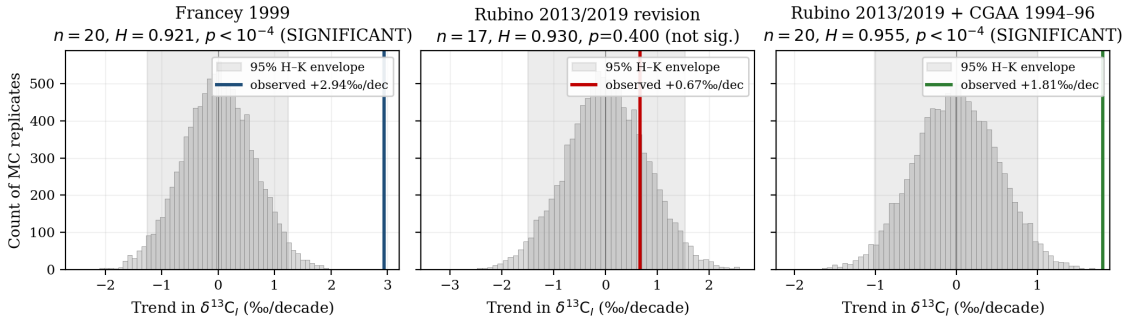


Figure 2: Recent-window trend against the H–K null distribution for each treatment. Gray histogram: 10 000 Monte Carlo replicates of the recent-window trend under a Gaussian fractional-noise null with the observed Hurst exponent. Shaded band: 95% envelope (the $[2.5, 97.5]$ percentile range of the Monte Carlo distribution). Colored line: trend on the data. On the primary data [7] and on Rubino + CGAA the trend sits outside the envelope in the positive direction, falsifying the fossil-dominance prediction of a strongly negative recent-window trend.

The sign of the trend is positive on every treatment. This is the primary robustness statement: the direction of the falsification is not sensitive to any data-provenance choice. The fossil-dominance hypothesis predicts a negative trend in the recent window; the trend is not negative on any of the three treatments.

The magnitude of the trend and its distinguishability from H–K noise vary with data treatment. On the two treatments that extend to 1996 the trend is significant at $p < 10^{-4}$. On the Rubino-alone treatment it is not, and Section 6 shows why.

6. The Rubino Endpoint Truncation

The only treatment on which the falsification does not achieve statistical significance is the Rubino et al. (2013) [15] revision on its own. This section documents that the failure is entirely an artifact of the endpoint truncation, and that restoring the three excluded CGAA years (which are on the same measurement chain Rubino did revise) recovers the falsification.

Comparing the Rubino-alone row of Table 2 with the Rubino + CGAA row: the trend rises from

+0.67 to +1.81‰ per decade when the three CGAA years are appended, and the 95% envelope narrows from [−1.50, +1.54] to [−1.01, +1.01]‰ per decade. Both effects contribute to the change in significance verdict, but the primary effect is on the trend statistic: those three years occupy the steepest part of the recent-window upward reversal. Their inclusion changes the significance verdict.

Section 4.2 establishes that the excluded samples share every element of the measurement chain with the samples Rubino revised: the same laboratory, the same instrument, the same working gas, the same calibration scale, the same admission scheme. The only difference is the source medium (Cape Grim tank versus Antarctic ice or firn). The scoping decision cannot be justified as a measurement-chain purification, because the measurement chain the two sets share is precisely the chain Rubino's revised procedures aim to improve.

The analytical consequence of the scoping decision, holding aside its stated justification, is to remove the three years in which the recent-window trend in $\delta^{13}C_I$ clears the H–K noise envelope. Any downstream analyst who cites Rubino as the current authoritative Law Dome record and applies the recent-window test to that record alone concludes that the recent-window trend is statistically indistinguishable from H–K noise. The same analyst applying the same test to the same measurement chain extended with three additional years from the same laboratory concludes that the falsification of fossil dominance stands at $p < 10^{-4}$.

The remedy is procedural. Any test of recent-window trend significance on the Law Dome $\delta^{13}C$-CO_2 record should use either Francey et al. (1999) [7] directly, or the Rubino record extended with the CGAA years from Francey et al. (1999) [7] Table 1. The two extended forms give equivalent falsification verdicts.

7. Discussion

7.1 Three complementary falsifications of fossil dominance from the isotopic record

The falsification established here is the third complementary line of isotopic evidence against the fossil-dominance hypothesis:

1. **Stationarity of $\delta^{13}C_I$ at −13.2‰ across five centuries.** Koutsoyiannis (2024) [13] demonstrates that the Keeling intercept $\delta^{13}C_I$ is stationary at -13.2 ± 0.2‰ across the 44-year Scripps four-site instrumental record, and stationary at approximately −13‰ across the five-century Caribbean sclerosponge proxy back to the Little Ice Age [2], with independent Law Dome ice-core confirmation [11]. A dominant fossil contribution would drift the intercept toward −28‰. It has not drifted.

2. **Algebraic bound $f \leq 0.013$ from the mass partition equation.** Cohler & Soon (2026a) [4] substitutes the observed stationary $\delta^{13}C_I \approx -13.2$‰ into Equation (2) with the standard empirically measured $\delta^{13}C$ values from the peer-reviewed literature and shows that the fossil fraction of the net atmospheric addition is bounded above by approximately 0.013, indistinguishable from zero at the precision of the intercept estimate. The bound follows from three inputs the IPCC endorses: mass conservation, the standard empirically measured $\delta^{13}C$ values, and the primary Scripps and sclerosponge datasets. The bound is inherited unchanged by any scenario operating on the same mass partition equation, including the proposed scenario in which non-fossil-fuel sources absorb approximately half of a putative fossil surplus: what controls $\delta^{13}C_I$ is the signature of the net input, not the molecular identity of what the atmosphere retains or the mechanism by which the remainder is removed.

3. **Statistically significant positive recent-window trend in $\delta^{13}C_I$** (this work). The trend in $\delta^{13}C_I$ over 1977–1996 on the primary Francey et al. (1999) [7] data is +2.94‰ per decade

against an H–K envelope of $[-1.26, +1.24]$‰ per decade, $p < 10^{-4}$. The sign contradicts the fossil-dominance prediction (Section 2.1), and the significance rules out the alternative that the positive trend is a statistical artifact of the noise background. This result is a direct empirical test of a sign prediction, not a restatement of the stationarity result in (i): the two statistics can in principle disagree (a monotone intercept drift with a sign-wrong recent-window trend is logically possible), and the data satisfy both constraints together.

Each of the three falsifications rests on the same primary datasets and the same standard empirically measured $\delta^{13}C$ values used throughout the carbon-cycle assessment literature. Each is derived by an elementary mathematical construction: a long-window Keeling regression for the stationary intercept, mass partition algebra for the f-bound, and a linear-trend fit on the pointwise fixed-$\Delta[CO_2]$ extraction with Monte Carlo significance for the recent-window falsification. None invokes a modeled quantity. Each is capable of standing alone. The three are three complementary consequences of applying the same isotopic construction to overlapping data through three different reduction procedures that each engage a different, independently falsifiable prediction of fossil dominance. Their agreement is a statement about the internal consistency of the isotopic evidence base.

The stationary object in (i) and (ii) is the long-window Keeling-plot intercept $\delta^{13}C_I^{long}$, an OLS fit through many years of paired $(\delta^{13}C, 1/C)$ observations; its ±0.2‰ uncertainty is the standard error of that long-baseline regression [13]. The trending object in (iii) is the pointwise fixed-$\Delta[CO_2]$ extraction defined by Equation (5), evaluated at each endpoint against the most recent prior year satisfying the $\sigma_{[CO_2]}$ criterion. The two objects share the same interpretation (flux-weighted mean signature of the net input) but resolve different timescales: the long-window intercept averages across the fit window, while the pointwise extraction retains the composition of the most recent multi-year addition. There is no arithmetic contradiction between a stationary long-window intercept at -13.2 ± 0.2‰ and a several-per-mil swing in the pointwise extraction within a short recent window; the two estimators measure different aspects of the same underlying source-mix history.

Together the three falsifications constrain the fossil fraction of the net atmospheric addition to approximately zero across the full record, in the specific direction (positive $\delta^{13}C_I$ trend) that the alternative non-fossil-fuel-source hypothesis predicts, and with the specific significance ($p < 10^{-4}$) that rules out the null of H–K noise.

7.2 The implied physical mechanism

The positive recent-window trend in $\delta^{13}C_I$ requires that the complement signature $\delta^{13}C_N$ be moving toward the less-negative standard ocean-outgassing $\delta^{13}C$ value during the recent window (Equation (2) with $f \approx 0$). Cohler & Soon (2026b) [5] develops the mechanism from first principles. Under a top-of-atmosphere radiative imbalance of approximately 2.6 W m^{-2}, ocean outgassing responds via van't Hoff surface-pCO_2 sensitivity ($\partial \ln pCO_2/\partial T \approx 0.0423$ K^{-1}) with an effective flux of approximately 2.44 GtC/yr, and biosphere respiration responds via Arrhenius $Q_{10} \approx 1.5$ with an effective flux of approximately 2.34 GtC/yr, matching the atmospheric growth of approximately 2.25 ppm/yr. Ocean outgassing acts on the entire surface ocean essentially instantly, while biosphere respiration is buffered by thermal inertia and biological turnover on decadal timescales. In the fastest-warming subperiod the ocean fraction of the enhanced non-fossil-fuel flux therefore grows relative to the biosphere fraction, and the flux-weighted mean $\delta^{13}C_N$ shifts toward the standard ocean-outgassing $\delta^{13}C$ value near −8‰. Under Equation (2) with $f \approx 0$, this drives $\delta^{13}C_I$ upward. The +2.94‰ per decade observed over 1977–1996 is what that shift produces under Equation (2).

The same mechanism explains the 1960–1975 declining subperiod in $\delta^{13}C_I$ that precedes the test window (Figure 1). The kinetic distinction is the key: ocean outgassing responds to the instan-

taneous surface temperature via van't Hoff, while biosphere respiration lags surface temperature through soil carbon-pool turnover on multi-decadal timescales. The 1960–1975 interval coincides with the well-documented mid-century pause in sustained sea-surface warming. Over that interval the van't Hoff ocean-outgassing driver weakened immediately, while the biosphere-respiration flux continued at a level set by the pool stock accumulated through the warmer 1930s–1940s. The flux-weighted mean $\delta^{13}C_N$ therefore shifted toward the more-negative biosphere-respiration signature (bulk respiration $\approx -27‰$ in a C3-dominated ecosystem) and $\delta^{13}C_I$ declined. The reversal at approximately 1977 coincides with the resumption of sustained sea-surface warming: ocean outgassing responds immediately, biosphere respiration remains buffered, the ocean fraction of the enhanced non-fossil-fuel flux grows, and $\delta^{13}C_I$ rises at the test-window rate. The sign of the trend in $\delta^{13}C_I$ tracks the sign of sustained sea-surface warming on timescales longer than the ocean-biosphere kinetic separation.

The positive-trend direction admits more than one physical realization. The temperature-driven ocean-outgassing mechanism developed here is the leading candidate, consistent with the first-principles flux-matching numbers above and with the kinetic distinction between instantaneous surface-ocean response and buffered biospheric response. Additional contributions in the same direction include a shift in the C3/C4 productivity ratio toward the less-negative standard C4 $\delta^{13}C$ value (greening in C4-dominated regions) and the secular decline in the global discrimination factor of C3 photosynthesis documented by Keeling et al. (2017) [10]. The sign prediction tested here does not distinguish between these candidates; what it falsifies is the hypothesis of fossil dominance.

The stationary intercept, the algebraic bound $f \approx 0$, and the positive recent-window trend are three observational consequences of one physical framework: non-fossil-fuel fluxes dominate the net atmospheric addition and their partition responds to surface warming.

7.3 Consequence for the downstream literature

The Rubino et al. (2013) [15] revision, and its Rubino et al. (2019) [16] update, are the currently cited authoritative Law Dome $\delta^{13}C$-CO_2 record in IPCC AR6 Chapter 5 [3] and in the NOAA/WDS Paleoclimatology archive. The revision omits the Cape Grim Air Archive samples that Francey et al. (1999) [7] included in Table 1, and its endpoint sits at 1993, three years before the 1996 endpoint of the underlying measurement chain. Any downstream analyst who tests recent-window trend significance on the Rubino record alone will find a non-significant trend and may conclude that the isotopic record does not contain a decisively significant recent-window signal in either direction. The same analyst using the primary Francey et al. (1999) [7] data, or the Rubino record extended with the three excluded years from Francey's Table 1, will find the falsification of fossil dominance at $p < 10^{-4}$.

The remedy is procedural, as noted in Section 6. Use the primary source directly, or extend the revision by the three years the revision excludes for scope reasons rather than measurement-chain reasons. Do not test recent-window significance on the truncated record alone.

8. Conclusion

The fossil-fuel dominance hypothesis for rising atmospheric CO_2, central to IPCC assessment [3] and reasserted in recent carbon-cycle attribution analyses [6], predicts a specific outcome on the highest-emissions window: a strongly negative recent-window trend in the flux-weighted mean signature $\delta^{13}C_I$ of the net atmospheric input, statistically distinguishable from the noise background of the extraction. On the primary Law Dome ice-core, firn, and Cape Grim Air Archive record of Francey et al. (1999) [7], we test this prediction directly using Equation 13 of Koutsoyiannis (2024) [13] with the fixed-$\Delta[CO_2]$ technique and a Hurst–Kolmogorov Monte

Carlo assessment of significance. The trend on 1977–1996 is +2.94‰ per decade against a 95% H–K envelope of $[-1.26, +1.24]$‰ per decade, with $p < 10^{-4}$. The trend is significant, positive, and of magnitude more than twice the noise-envelope bound. The fossil-dominance hypothesis is falsified on the isotopic record cited as authoritative in the assessment literature.

Together with the stationarity and algebraic-bound results reviewed in Section 7.1, this trend forms the third of three isotopic constraints that jointly place the fossil fraction of the net atmospheric addition at approximately zero. The positive sign of the trend is the direction the temperature-driven ocean-and-biosphere mechanism of Section 7.2 predicts, and the significance rules out the H–K-noise null. The direction is robust across data treatments; the only treatment on which significance is lost, the Rubino revision on its own, fails through an endpoint truncation that removes the three CGAA years on the same CSIRO GASLAB measurement chain Rubino retains for the ice and firn samples.

Data Used

The Francey et al. (1999) [7] Tables 1–3 are reproduced from the open-access reissue at: https://b.tellusjournals.se/articles/10.3402/tellusb.v51i2.16269

The Rubino Law Dome CO_2 and $\delta^{13}C$ files [15, 16] are archived at NOAA/WDS Paleoclimatology: https://www.ncei.noaa.gov/pub/data/paleo/icecore/antarctica/law/

Funding

This work received no external funding.

Co-Editor: Demetris Koutsoyiannis; Reviewers: anonymous

Acknowledgments

The authors thank Demetris Koutsoyiannis for the foundational $\delta^{13}C_I$ construction on which this analysis builds. The authors used Claude Opus 4.7 (Anthropic) and Grok 4.7 (xAI) as computational and writing aids during preparation. All scientific claims, derivations, numerical inputs, and conclusions were independently verified by the authors, who take full responsibility for the content of this work and for any errors or omissions.

The views expressed in this work are solely those of the authors and do not represent the views of any affiliated institution.

Conflict of Interest

The authors declare no conflict of interest.

References

[1] Andres, R. J., Marland, G., Boden, T., & Bischof, S. (2000). Carbon dioxide emissions from fossil fuel consumption and cement manufacture, 1751–1991; and an estimate of their isotopic composition and latitudinal distribution. In T. M. L. Wigley & D. S. Schimel (Eds.), *The carbon cycle* (pp. 53–62). Cambridge University Press.

[2] Böhm, F., Haase-Schramm, A., Eisenhauer, A., Dullo, W.-C., Joachimski, M. M., Lehnert, H., & Reitner, J. (2002). Evidence for preindustrial variations in the marine surface water carbonate system from coralline sponges. *Geochemistry, Geophysics, Geosystems*, 3(3), 1019.

[3] Canadell, J. G., Monteiro, P. M. S., Costa, M. H., Cotrim da Cunha, L., Cox, P. M., Eliseev, A. V., Henson, S., Ishii, M., Jaccard, S., Koven, C., Lohila, A., Patra, P. K., Piao, S., Rogelj, J., Syampungani, S., Zaehle, S., & Zickfeld, K. (2021). Global carbon and other biogeochemical cycles and feedbacks. In V. Masson-Delmotte et al. (Eds.), *Climate Change 2021: The Physical Science Basis. Contribution of Working Group I to the Sixth Assessment Report of the Intergovernmental Panel on Climate Change* (pp. 673–816). Cambridge University Press.

[4] Cohler, J., & Soon, W. (2026a). Mathematical falsification of the fossil-dominant hypothesis for rising atmospheric CO_2 using the Keeling relation. *Science of Climate Change*, in press.

[5] Cohler, J., & Soon, W. (2026b). Dominance of natural atmospheric CO_2 dynamics: Falsification of anthropogenic attribution through mass-balance analysis, isotopic diagnostics, and thermodynamic first principles. Manuscript submitted for publication. https://papers.jcohler.com/co2

[6] Engelbeen, F., Hannon, R., & Burton, D. (2024). *The Human Contribution to Atmospheric Carbon Dioxide: How Human Emissions Are Restoring Vital Atmospheric CO_2*. CO_2 Coalition.
https://doi.org/10.5281/zenodo.14231820

[7] Francey, R. J., Allison, C. E., Etheridge, D. M., Trudinger, C. M., Enting, I. G., Leuenberger, M., Langenfelds, R. L., Michel, E., & Steele, L. P. (1999). A 1000-year high precision record of $\delta^{13}C$ in atmospheric CO_2. *Tellus B*, 51(2), 170–193.

[8] Friedlingstein, P., O'Sullivan, M., Jones, M. W., et al. (2026). Global Carbon Budget 2025. *Earth System Science Data*, 18, 3211–3288.

[9] Keeling, C. D. (1958). The concentration and isotopic abundances of atmospheric carbon dioxide in rural areas. *Geochimica et Cosmochimica Acta*, 13, 322–334.

[10] Keeling, R. F., Graven, H. D., Welp, L. R., Resplandy, L., Bi, J., Piper, S. C., Sun, Y., Bollenbacher, A., & Meijer, H. A. J. (2017). Atmospheric evidence for a global secular increase in carbon isotopic discrimination of land photosynthesis. *Proceedings of the National Academy of Sciences*, 114(39), 10361–10366.

[11] Köhler, P., Fischer, H., Schmitt, J., & Munhoven, G. (2006). On the application and interpretation of Keeling plots in paleo climate research—deciphering $\delta^{13}C$ of atmospheric CO_2 measured in ice cores. *Biogeosciences*, 3(4), 539–556.

[12] Kohn, M. J. (2010). Carbon isotope compositions of terrestrial C3 plants as indicators of (paleo)ecology and (paleo)climate. *Proceedings of the National Academy of Sciences*, 107, 19691–19695.

[13] Koutsoyiannis, D. (2024). Net isotopic signature of atmospheric CO_2 sources and sinks: No change since the Little Ice Age. *Sci*, 6(1), 17.

[14] Mook, W. G. (1986). ^{13}C in atmospheric CO_2. *Netherlands Journal of Sea Research*, 20, 211–223.

[15] Rubino, M., Etheridge, D. M., Trudinger, C. M., Allison, C. E., Battle, M. O., Langenfelds, R. L., Steele, L. P., Curran, M., Bender, M., White, J. W. C., Jenk, T. M., Blunier, T., & Francey, R. J. (2013). A revised 1000 year atmospheric $\delta^{13}C$-CO_2 record from Law Dome and South Pole, Antarctica. *Journal of Geophysical Research: Atmospheres*, 118(15), 8482–8499.

[16] Rubino, M., Etheridge, D. M., Thornton, D. P., Howden, R., Allison, C. E., Francey, R. J., Langenfelds, R. L., Steele, L. P., Trudinger, C. M., Spencer, D. A., Curran, M. A. J., van Ommen, T. D., & Smith, A. M. (2019). Revised records of atmospheric trace gases CO_2, CH_4, N_2O, and $\delta^{13}C$-CO_2 over the last 2000 years from Law Dome, Antarctica. *Earth System Science Data*, 11(2), 473–492.

[17] Zhang, J., Quay, P. D., & Wilbur, D. O. (1995). Carbon isotope fractionation during gas-water exchange and dissolution of CO_2. *Geochimica et Cosmochimica Acta*, 59, 107–114.

Disclaimer/Publisher's Note:

This article reflects solely the views, analyses, and conclusions of the author(s). Science of Climate Change, its editors, and its publisher make no representation or warranty as to the accuracy or completeness of the content and disclaim liability for any loss, damage, or other consequence arising from the use of, or reliance on, any material published herein.